Theoretical analysis of the second-harmonic light power in a biaxial crystal

Guohui Li (李国辉), Jie Ye (叶 捷), and Xinye Xu (徐信业)*

State Key Laboratory of Precision Spectroscopy and Department of Physics, East China Normal University, Shanghai 200062, China

**E-mail: xyxu@phy.ecnu.edu.cn*

Received December 10, 2009

Theoretical analyses are presented on the critically phase-matched second-harmonic generation (SHG) in a biaxial crystal with the focused fundamental Gaussian beams. The dependence of the second-harmonic light power on the phase matching conditions, focused geometries, walk-off effects, and absorptions are discussed in detail. Expressions are presented for calculating the light power of the types I and II SHGs in the biaxial crystal, applied to optimize the blue light generation with the LiB_3O_5 crystal. A maximum conversion efficiency of around 37% is obtained with 798-nm laser power of 500 mW.

OCIS codes: 190.2620, 140.3515, 160.4330, 140.3560.

doi: *10.3788/COL20100807.0693.*

Second-harmonic generation (SHG) of light has numerous important applications in nonlinear optics[1−4], aside from being a highly efficient way to generate the blue and green lasers for studies in the field of precision spectroscopy, atom cooling and trapping, and quantum optics[5,6]. Theoretical works have been done on the optimization of SHG with the focused fundamental Gaussian beam in a uniaxial nonlinear crystal[7,8]. These works have been extended to type I SHG with elliptical fundamental Gaussian beams[9]. Biaxial nonlinear crystals that have higher damage threshold, broader transparency range, and relatively larger effective nonlinear coefficients are also frequently used in SHG. As opposed to a uniaxial crystal, the situation in a biaxial crystal, in which the three crystal axes have different refractive indices is more complex and has many configurations[10,11]. Likewise, the walk-off angles are different depending on the angular coordinates in the critical direction. However, all these configurations in a biaxial crystal can be categorized in two: type I and type II SHGs[12]. Studies have been done on the phase-matching conditions and double refraction walk-off angles of SHG in a biaxial crystal. Kerkoc *et al.* have made the corresponding extensions of the former theory of SHG in a uniaxial crystal with focused fundamental Gaussian beams to include a biaxial crystal—MBANP[13].

However, the previous analyses generally referred to specific experimental situations. Hence, a comprehensive study of critically phase-matched SHG in a biaxial nonlinear crystal is highly important. In this letter, we extend the theory further for the analyses of types I and II SHGs with the focused fundamental Gaussian beams in biaxial crystals. The treatment presented here leads to the results of general significance as a function of the crystal parameters, from which optimally focused geometries can be found and theoretical estimation of the SHG power can be made. As an example, we apply the result to optimize the SHG of a diode laser at 798 nm in a LiB_3O_5 (LBO) crystal.

We followed the notations of the classic paper of Boyd and Kleinman (BK)[7] in the calculations but presented our results in SI units. The biaxial nonlinear crystal with the length l was cut to satisfy the ordinary phase matching condition Δk=$2k_1$–k_2=0, where the wave vector of the fundamental (second harmonic, SH) light is represented by $k_1(k_2)$. In type I SHG, the two fundamental waves have parallel polarizations. According to the theory of Brehat *et al.*[12], type I SHG in a biaxial crystal in laboratory coordinates can be generalized as the configuration shown in Fig. 1; the relationship between the laboratory axes (x, y, z) and the crystallographic axes (X, Y, Z) can be found in Ref. [14]. The light propagation direction is along the z axis, and its origin is at the crossing point of the light beam and the front facet of the nonlinear crystal. The double refraction angle for the fundamental (SHG) extraordinary waves is $\mathrm{d}x/\mathrm{d}z=\tan\rho_\omega \approx \rho_\omega$ ($\mathrm{d}y/\mathrm{d}z=\tan\rho_{2\omega} \approx \rho_{2\omega}$) (Fig. 1). The fundamental beam is a Gaussian beam with a focus of $z = f$ characterized by the beam waist w_0, confocal parameter b, and diffraction half-angle δ_0. These satisfy the relations $w_0^2 k_1 = b$ and $\delta_0=2w_0/b=2/(bk_1)^{1/2}$. Therefore, the electric field of a fundamental light beam propagating in the crystal like an extraordinary beam can be written as[7]

$$E_\omega(x,y,z) = E_0(1+\mathrm{i}\tau)^{-1}\exp(\mathrm{i}k_1 z - \mathrm{i}\omega_1 t) \times \exp\left\{-\frac{[x-\rho_\omega(z-f)]^2+y^2}{w_0^2(1+\mathrm{i}\tau)}\right\} \times \exp\left(-\frac{1}{2}a_1 z\right), \quad (1)$$

where τ=$2(z$–$f)/b$, E_0 is a constant, and a_1 and ω_1 are the absorption coefficient and the angular frequency of the fundamental field, respectively.

We then calculated the SH field $E_{2\omega}(x_1, y_1, z_1)$ at the observer point $P(x_1, y_1, z_1)$. The walk-off of the fundamental field has been taken into account in Eq. (1). The relationship between the source point $R(x, y, z)$ and the observer point $P(x_1, y_1, z_1)$ are $y = y_1 - \rho_{2\omega}(z_1 - z)$, $(z_1 < l)$; $y = y_1 - \rho_{2\omega}(l - z)$, $(z_1 > l)$; $x = x_1$, $(0 \le z \le l)$ (Fig. 1). Then, the electric field of the SH light at the observer point outside the crystal is

$$E_{2\omega}(x_1,y_1,z_1) = \frac{\mathrm{i}\omega_1 d E_0^2}{cn_2(1+\mathrm{i}\tau')} \times \exp(-a_2 l/2 + 2\mathrm{i}k_1 z_1 - 2\mathrm{i}\omega_1 t) \times \int_0^l \mathrm{d}z \frac{\exp(-az+\mathrm{i}\Delta kz)}{1+\mathrm{i}\tau} \exp\left\{-2\frac{[x_1-\rho_\omega(z-f)]^2+[y_1-\rho_{2\omega}(l-z)]^2}{w_0^2(1+i\tau')}\right\}, \quad (2)$$

where a_2 is the absorption coefficient for the SH light in the crystal, d is the effective nonlinear coefficient, $a = a_1 - a_2/2$, and $\tau' = 2(z_1 - f)/b$.

The intensity of the SH light in the far field ($\tau' \to \infty$) outside the crystal is

$$I = \frac{1}{2}\varepsilon_0 c n_2 |E_{2\omega}|^2 = \frac{8P_1^2 d^2 \omega_1^2 k_1^2}{\varepsilon_0 c^3 n_1^2 n_2 \tau'^2} \exp(a\mu l) \times \exp(-a'l) \times \exp[-4(s^2+s'^2)]|H|^2, \quad (3)$$

where $s = x_1/(w_0\tau')$, $s' = [y_1 - \rho_{2\omega}(l-f)]/(w_0\tau')$, $a' = a_1 + a_2/2$, the focal position is $\mu = (l-2f)/l$, and

$$H = \frac{1}{2\pi}\int_{-\xi(1-\mu)}^{\xi(1+\mu)} \mathrm{d}\tau \frac{\exp(-\kappa\tau + \mathrm{i}\sigma'\tau)}{1+\mathrm{i}\tau}. \quad (4)$$

In the above, $\sigma' = \sigma - 4(\beta_1 s - \beta_2 s')$, the phase mismatching parameter σ is defined as $\sigma = b\Delta k/2$, the focusing parameter ξ is defined as $\xi = l/b$, and $\kappa = ab/2$.

By integrating the SHG intensity, the SH light power can be written as

$$P_{2\omega} = \frac{2P_1^2 d^2 \omega_1^2}{\varepsilon_0 c^3 n_1^2 n_2 \pi} k_1 l \exp(-a'l) \times h(\sigma, B, \kappa, \xi, \mu), \quad (5)$$

where the BK factor is

$$h(\sigma,B,\kappa,\xi,\mu) = \frac{1}{4\xi}\exp(\mu a l)\int\int_{-\xi(1-\mu)}^{\xi(1+\mu)} \mathrm{d}\tau'\mathrm{d}\tau \cdot \frac{\exp[-\kappa(\tau+\tau') + \mathrm{i}\sigma(\tau'-\tau) - B^2(\tau'-\tau)^2/\xi]}{(1+\mathrm{i}\tau')(1-\mathrm{i}\tau)}. \quad (6)$$

In the above, $B^2 = B_1^2 + B_2^2$. The double-refraction parameter B_1 (B_2) is defined as $B_1 = \rho_\omega (lk_1)^{1/2}/2$ ($B_2 = \rho_{2\omega}(lk_1)^{1/2}/2$). The double refraction parameter (B) in the type I SHG consists of two terms (B_1, B_2) because two extraordinary axes exist in the biaxial crystal, and, in contrast, just one extraordinary axis exists in the uniaxial crystal, as shown in Eq. (5). For type I SHG in a negative (positive) uniaxial crystal, in which the double-refraction parameter $B = B_2$ ($B = B_1$), the result agrees with that presented in Ref. [7].

According to the phase-matching theory, fundamental waves are formed by orthogonally polarized lights (E_ω and E'_ω) in type II SHG. The configuration of the type II SHG in the biaxial crystal can be generalized and are presented in Fig. 2[12]. The beam propagation directions are along the z axis. The double refraction directions for the fundamental waves are $\mathrm{d}x/\mathrm{d}z = \tan\rho_1 \approx \rho_1$ and $\mathrm{d}y'/\mathrm{d}z = \tan\rho_2 \approx \rho_2$. For the SHG wave, it is $\mathrm{d}y/\mathrm{d}z = \tan\rho_{2\omega} = \rho_{2\omega}$.

In type II SHG, the fundamental electric field is composed of two orthogonally polarized components (E_ω, E'_ω). In Fig. 2, the fundamental electric fields (E_ω, E'_ω) in the crystal can be expressed as

$$E_\omega(x,y,z) = E_0(1+\mathrm{i}\tau)^{-1}\exp(\mathrm{i}k_1 z - \mathrm{i}\omega_1 t) \times \exp\left\{-\frac{[x-\rho_1(z-f)]^2+y^2}{w_0^2(1+\mathrm{i}\tau)}\right\} \times \exp\left(-\frac{1}{2}a_1 z\right), \quad (7a)$$

and

$$E'_\omega(x,y,z) = E_0(1+\mathrm{i}\tau)^{-1}\exp(\mathrm{i}k_1 z - \mathrm{i}\omega_1 t) \times \exp\left\{-\frac{x^2+[y+\rho_2(z-f)]^2}{w_0^2(1+\mathrm{i}\tau)}\right\} \times \exp\left(-\frac{1}{2}a_1 z\right), \quad (7b)$$

Then, the electric field of the SH light at the observer point $P(x_1, y_1, z_1)$ in type II SHG is calculated. As the two fundamental fields have different polarizations, we assume two source points (R_1, R_2) as shown in Fig. 2. At the same time, the walk-offs of the fundamental fields have been taken into account in Eq. (7). Therefore, the observer point $P(x_1, y_1, z_1)$ and the source points $R_1(x, y, z)$ and $R_2(x, y, z)$ satisfy $y = y_1 - \rho_{2\omega}(z_1 - z)$, ($z_1 < l$); $y = y_1 - \rho_{2\omega}(l-z)$, ($z_1 > l$); $x = x_1$, ($0 \le z \le l$). The electric field of the SH light outside the crystal is

$$E_{2\omega}(x_1,y_1,z_1) = \frac{\mathrm{i}\omega_1 d E_0^2}{cn_2(1+\mathrm{i}\tau')} \times \exp(-a_2 l/2 + 2\mathrm{i}k_1 z_1 - 2\mathrm{i}\omega_1 t) \times \int_0^l \mathrm{d}z \frac{\exp(-az+\mathrm{i}\Delta kz)}{1+\mathrm{i}\tau} \times \exp\left\{-\frac{[x_1-\rho_1(z-f)]^2+[y_1-\rho_{2\omega}(l-z)]^2+x_1^2+[y_1-\rho_{2\omega}(l-z)+\rho_2(z-f)]^2}{w_0^2(1+\mathrm{i}\tau')}\right\}. \quad (8)$$

Therefore, the SH power in the far field ($\tau' \to \infty$) outside the crystal is

$$P_{2\omega} = \frac{2P_1^2 d^2 \omega_1^2}{\varepsilon_0 c^3 n_1^2 n_2 \pi} k_1 l \exp(-a'l) \times h(\sigma, B, \kappa, \xi, \mu). \quad (9)$$

Here, $B^2 = B_3^2 + B_2 B_3 + B_2^2/4 + B_1^2/4$. The double refraction parameters are defined as $B_1 = \rho_1(lk_1)^{1/2}/2$, $B_2 = \rho_2(lk_1)^{1/2}/2$, and $B_3 = \rho_{2\varpi}(lk_1)^{1/2}/2$. As can be seen from Eq. (9), the double-refraction parameter B in the type II SHG is more complicated than that in the type I SHG. The difference is caused by the different double refraction directions of the orthogonally polarized fundamental waves in type II SHG.

To realize Yb lattice clock, it is essential that 399 nm

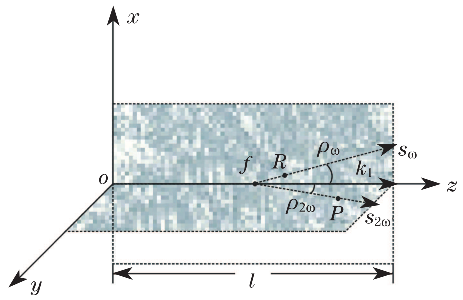

Fig. 1. Type I phase-matched SHG in a biaxial crystal in laboratory coordinates (x, y, and z). s_ω ($s_{2\omega}$) is the energy flow direction of the fundamental (SH) wave, ρ_ω ($\rho_{2\omega}$) is the walk-off angle of the fundamental (SH) wave, R (P) is the source (observer) point, k_1 is the propagation direction of the fundamental light, and f is the focus of the fundamental Gaussian beam.

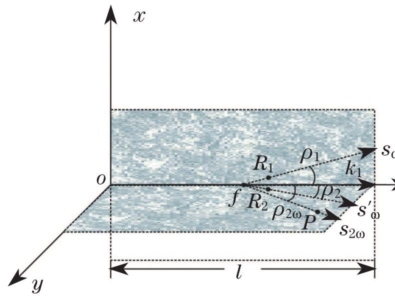

Fig. 2. Type II SHG in a biaxial crystal in laboratory coordinates (x, y, and z). s_ω, s'_ω, and $s_{2\omega}$ are the energy flow directions of fundamental fields E_ω and E'_ω, and SHG field $E_{2\omega}$, respectively; R_1 and R_2 are the source points; P is the observer point; ρ_1, ρ_2, and $\rho_{2\omega}$ are the corresponding walk-off angles; and f is the focus of the fundamental Gaussian beam.

$^1S_0-^1P_1$ broad line transition is used to cool and trap Yb atoms[15−17]. The PPKTP and LBO crystals are the possible candidates for generating a 399-nm laser. Villa *et al.* have achieved high-efficient blue light generation with PPKTP[6]; however, thermal lensing and bistability appeared in the experiment when the fundamental power surpassed 300 mW. The LBO widely used for blue and green light generation is a typical biaxial crystal. Compared with the PPKTP crystal, it has higher optical homogeneity, higher damage threshold, and broader transparency range resulting in low loss for both the 399- and 798-nm laser lights. Therefore, we adopted frequency doubling of a diode laser using the LBO crystal to generate light source at 399 nm. To minimize surface losses, Brewster-cut LBO crystal was used in the design because of the following advantages: minimum residual reflections on both facets, larger damage threshold, and longer lifetime compared with the anti-reflection (AR) coated LBO crystal[18]. In the following, we applied the theory to analyze blue 399-nm light generation in a biaxial crystal. The calculations were performed for a 3×3×12 (mm) crystal.

SHG is the most efficient when it is phase matched. According to the refractive indices in Table 1, the maximum nonlinearity can be achieved at type I phase matching with θ=90° and $\varphi \approx$31.9°[10,11], where θ is the angle between the wave propagation direction and Z axis, and φ is the angle between the projection of wave propagation direction in X-Y plane and X axis.

Table 1. Refractive Indices at the Fundamental Laser Frequency ω (797.822 nm) and the SHG Laser Frequency 2ω (398.911 nm) in the Crystallographic Coordinates (X, Y, Z)

λ(nm)	n_X	n_Y	n_Z
798	1.569	1.596	1.611
399	1.590	1.619	1.635

Table 2. Optimal Configuration for Efficient SHG from 798 to 399 nm

θ(deg.)	φ(deg.)	d(pm/V)	ρ_ω(mrad)	$\rho_{2\omega}$(mrad)
90	31.9	0.712	16.7	31.1

After phase matching, the refractive indices of both fundamental and SH lights are 1.611, hence obtaining a Brewster angle of ϕ=58.17°. The magnitudes of walk-off angles are shown in Table 2, and the details of the calculation can be found in Ref. [12]. We will use Eq. (5) for type I phase-matched SHG in a biaxial crystal in the following optimizations and calculations.

With the data shown in Table 2, the BK factor in Eq. (5) can be plotted in Fig. 3. We find that the maximum value of $h(\xi)$ is 0.101 at $\xi \sim$1.5, indicating that the optimal beam waist of the fundamental beam is around 25 μm. Given the small nonlinearity of the LBO crystal, we chose to enhance the fundamental field in a four-mirror ring cavity. Compared with a semi-monolithic resonator, this configuration can avoid feedback to the laser diode and manifests low loss[18].

Figure 4 shows that the M1 and M2 cavities are flat mirrors, and that M3 and M4 are concave mirrors with the same radius of curvature of R_c. Here, M1 is the input coupler, M4 is the output coupler, and the length of the crystal is l. The cavity can be analyzed in terms of $ABCD$ matrix method[19]. The radius of curvatures of the two concave mirrors was chosen as R_c=70 mm. Given that the angle-tuned phase matching and the Brewster-cut surfaces in the design can cause astigmatism[9,18], we compensated for this by making the folding angle θ (as formed by the light ray and the surface normal of the concave mirror), thereby satisfying the relation $R_c \tan\theta \sin\theta = l(n^2-1)/n^3$[18], where n is the refractive index, and θ=14.57°.

From the theory of Ashkin *et al.*[20], we learned that the largest SHG conversion efficiency can be obtained when the cavity is impedance matched. Mirrors M2, M3, and

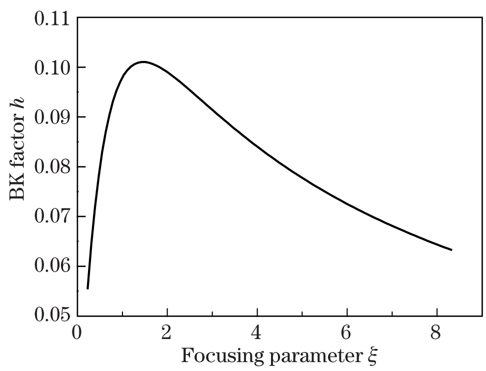

Fig. 3. BK factor h for the critically phase-matched SHG as a function of the focusing parameter ξ.

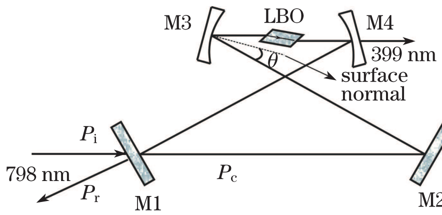

Fig. 4. Setup of the ring cavity for the SHG in the LBO crystal. M1, M2, M3, and M4 are the cavity mirrors; $P_{\rm i}$ is the input fundamental light power; $P_{\rm r}$ is the fundamental light power reflected by the cavity; and $P_{\rm c}$ is the fundamental light power inside the cavity.

M4 were selected with a high reflectivity of 99.97% for the fundamental light, and M4 has a transmission coefficient of up to 94% for the SH light. Generally, the absorption at 798 nm is estimated to be a_1 ∼0.31%/cm, the absorption at 399 nm is estimated to be a_2 <0.1%/cm[21], and the crystal loss at fundamental wavelength is around 0.45%[5]. As the output facet of the LBO crystal is Brewster-cut for 798 nm, the transmissivity of the crystal for 399 nm, $t_{\rm c}$, is around 80.3%[22]. To achieve the impedance matching condition, the optimal reflectivity r_m of M1 is around 99.4%; the ratio of the light power in the impedance matched cavity P_{cm} to the incident light power $P_{\rm i}$ can be represented as[20]

$$\frac{P_{cm}}{P_{\rm i}} = \frac{1}{1-r_m}. \qquad (10)$$

Substituting P_{cm} into Eq. (5), the SHG output power outside the resonant cavity $P_{\rm SHG}$ becomes

$$P_{\rm SHG} = KP_{cm}^2 lk_1 \exp(-a'l)\cdot h(\kappa,\sigma,B,\xi)t_2t_{\rm c}, \qquad (11)$$

where t_2 is the transmission coefficient of the output coupler and $K{=}2\omega_1^2 d^2/(\varepsilon_0 c^3 n_1 n_2 \pi)$. We defined the SHG conversion efficiency η as $\eta{=}P_{\rm SHG}/P_{\rm i}$.

The SHG conversion efficiency can be estimated from Eq. (11); through the *ABCD* matrix, we designed a resonator with the required waist inside the crystal and achieved a maximum BK factor $h(\xi)$=0.101. In the calculation, the fundamental light power $P_{\rm i}$ refers to the light power which is mode-matched into the cavity. Substituting all the parameters into Eq. (11), blue light generation of 188 mW at 399 nm could be generated with 500-mW mode-matched light power at 798 nm, and is equal to a conversion efficiency of around 37%.

In conclusion, we present a theoretical analysis for both types I and II phase-matched SHGs in a biaxial nonlinear crystal. Specific phase-matching conditions, polarizations of laser beams, and corresponding walk-off effects are analyzed. As a result, the dependence of SHG power in the biaxial crystal on these parameters is clarified. Such an analysis provides a theoretical and practical guidance for determining the optimum operating condition and estimation of SHG conversion efficiency in biaxial nonlinear crystals. As an example, we optimize the SHG in a typical biaxial crystal in the form of a LBO crystal. A 188-mW laser light emission at 399 nm could be efficiently generated with 500-mW mode-matched fundamental light power, suitable for cooling and trapping Yb atoms.

This work was supported by the National Natural Science Foundation of China (No. 10774044), the National Key Basic Research and Development Program of China (No. 2006CB921104), the Science and Technology Commission of Shanghai Municipality of China (No. 07JC14019), the Shanghai Pujiang Talent Program of China (No. 07PJ14038), and the PhD Program Scholarship Fund of East China Normal University (ECNU) 2009 (No. 2009049).

References

1. Z. Y. Ou, S. F. Pereira, E. S. Polzik, and H. J. Kimble, Opt. Lett. **17,** 640 (1992).
2. Y. Song, P. Zhang, X. Zhang, B. Yan, Y. Zhou, Y. Bi, and Z. Zhang, Chin. Opt. Lett. **6,** 271 (2008).
3. C. Zhou, L. Le Xuan, A. Slablab, N. Sandeau, S. Brasselet, D. Chauvat, and J.-F. Roch, Chin. Opt. Lett. **6,** 64 (2008).
4. S. Rong, X. Zhu, and W. Chen, Chin. Opt. Lett. **7,** 43 (2009).
5. B. Beier, D. Woll, M. Scheidt, K.-J. Boller, and R. Wallenstein, Appl. Phys. Lett. **71,** 315 (1997).
6. F. Villa, A. Chiummo, E. Giacobino, and A. Bramati, J. Opt. Soc. Am. B **24,** 576 (2007).
7. G. D. Boyd and D. A. Kleinman, J. Appl. Phys. **39,** 3597 (1968).
8. G. D. Boyd, A. Ashkin, J. M. Dziezic, and D. A. Kleinman, Phys. Rev. **137,** A1035 (1965).
9. T. Freegarde, J. Coutts, J. Walz, D. Leibfried, and T. W. Hänsch, J. Opt. Soc. Am. B **14,** 2010 (1997).
10. M. V. Hobden, J. Appl. Phys. **38,** 4365 (1967).
11. J. Q. Yao and T. S. Fahlen, J. Appl. Phys. **55,** 65 (1984).
12. F. Brehat and B. Wyncke, J. Phys. B: At. Mol. Opt. Phys. **22,** 1891 (1989).
13. P. Kerkoc, R. T. Bailey, F. R. Cruickshank, and D. Pugh, J. Opt. Soc. Am. B **15,** 438 (1998).
14. M. A. Dreger and J. H. Erkkila, Opt. Lett. **17,** 787 (1992).
15. Z. W. Barber, C. W. Hoyt, C. W. Oates, L. Hollberg, A. V. Taichenachev, and V. I. Yudin, Phys. Rev. Lett. **96,** 083002 (2006).
16. S. G. Porsev, A. Derevianko, and E. N. Fortson, Phys. Rev. A **69,** 021403 (2004).
17. C. Y. Park and T. H. Yoon, Phys. Rev. A **68,** 055401 (2003).
18. J. Hald, Opt. Commun. **197,** 169 (2001).
19. H. Kogelnik and T. Li, Appl. Opt. **5,** 1550 (1966).
20. A. Ashkin, G. D. Boyd, and J. M. Dziedzic, IEEE J. Quantum Electron. **2,** 109 (1966).
21. S. P. Velsko, M. Webb, L. Davis, and C. Huang, IEEE J. Quantum Electron. **27,** 2182 (1991).
22. E. Jurdik, J. Hohlfeld, A. F. van Etteger, A. J. Toonen, W. L. Meerts, H. van Kempen, and Th. Rasing, J. Opt. Soc Am. B **19,** 1660 (2002).